Research Square

Preprints are preliminary reports that have not undergone peer review.
They should not be considered conclusive, used to inform clinical practice,
or referenced by the media as validated information.

GIS-Based Agricultural Potential Zoning Using Remote Sensing Indicators and the Analytic Hierarchy Process: A Case Study of Blida Wilaya, Northern Algeria

Sarah Debbagh

saradebbagh16@gmail.com

University of Sciences and Technology Houari Boumediene

Ammar Lachehab

University of Sciences and Technology Houari Boumediene

Research Article

Keywords: Agricultural land suitability, GIS, Remote sensing, Analytic Hierarchy Process, Landsat 8, AUC/ROC validation, Blida, Algeria

Posted Date: November 13th, 2026

DOI: https://doi.org/10.21203/rs.3.rs-11473908/v1

License: This work is licensed under a Creative Commons Attribution 4.0 International License.
Read Full License

Additional Declarations:
No competing interests reported.

Tables 1 to 3 are available in the Supplementary Files section.

GIS-Based Agricultural Potential Zoning Using Remote Sensing Indicators and the Analytic Hierarchy Process: A Case Study of Blida Wilaya, Northern Algeria

Affiliations

DEBBAGH Sarah [1*]. LACHEHAB Ammar [2]

[1] *DEBBAGH Sarah, Laboratory of Geography and Planning, Faculty of Earth Sciences, Departement of Geography and Territorial Planning, University of Sciences and Technology Houari Boumediene (USTHB), Algiers, Algeria, saradebbagh16@gmail.com*

[2] *LACHEHAB Ammar, Laboratory of Geography and Planning, Faculty of Earth Sciences, Departement of Geography and Territorial Planning, University of Sciences and Technology Houari Boumediene (USTHB), Algiers, Algeria, ammarlachehab@yahoo.fr*

Acknowledgments

The authors sincerely thank the reviewers for their insightful comments and constructive suggestions, which significantly improved the quality and clarity of this paper.

Funding source

The authors declare that no funds, grants, or other financial support were received for the design, execution, and publication of this study.

Competing interest

All authors declare no competing interests.

Author contributions

Sarah Debbagh conceived and designed the study, developed the research methodology, prepared all figures and tables, and wrote the original draft of the manuscript and supervised the overall project. Ammar Lachehab, as supervisor, refined the research question and the methodological framework, verified the weight derivations and consistency ratios, contributed regional and field knowledge of the Blida-Mitidja-Atlas system, provided laboratory and institutional resources, and critically reviewed and edited the manuscript. Both authors read and approved the final manuscript and agree to be accountable for all aspects of the work.

Abstract

Agricultural land suitability assessment is a critical instrument for sustainable land-use planning in Mediterranean semi-arid regions exposed to climate variability, land degradation, and expanding urban pressure. This study develops and validates a GIS–remote sensing–based agricultural potential zoning (APZ) model for Blida Wilaya, northern Algeria, by integrating five spatial criteria: the Soil Moisture Index (SMI), the Normalized Difference Vegetation Index (NDVI), Land Surface Temperature (LST), Land Use/Land Cover (LULC), and a composite Agro-Physiographic Suitability factor derived from slope, elevation, and distance from water bodies. Multi-source datasets—Landsat 8 OLI/TIRS imagery acquired during the 2025 growing season, SRTM DEM, and OpenStreetMap hydrography—were harmonized to a 30 m grid on the Google Earth Engine platform and integrated within ArcGIS 10.8. Criterion weights were derived through the Analytic Hierarchy Process (AHP) eigenvector method, with SMI (0.4502) and NDVI (0.2502) exerting dominant influence; consistency ratios of 6.25% and 3.34% for the five-factor and three-factor matrices, respectively, confirmed the logical coherence of the elicited judgments. Weighted linear combination yielded a five-class APZ map covering 148,046 ha, of which 47.40% was classified as suitable, 22.53% as moderately suitable, 12.58% as highly suitable, 11.43% as marginally suitable, and 6.05% as not suitable. ROC validation produced an area under the curve of 0.935, indicating excellent discriminatory performance. The results delineate a suitable agricultural matrix across the Mitidja plain, a highly suitable belt along the Blidean Atlas front that should be interpreted as conservation-oriented

rather than as a mandate for intensification, and an urbanized piedmont corridor whose 4,015 ha of residual suitable land constitutes a finite reserve requiring explicit protection against urban sprawl. The framework provides a transparent, reproducible screening tool for sustainable agricultural planning in semi-arid Mediterranean landscapes.

Keywords: Agricultural land suitability; GIS; Remote sensing; Analytic Hierarchy Process; Landsat 8; AUC/ROC validation; Blida; Algeria

Introduction

Ensuring global food security and sustainable agricultural development has become increasingly challenging due to the compounded effects of climate variability, land-use change, and population growth. The Mediterranean basin and North African regions, including Algeria, are particularly vulnerable to these pressures, experiencing heightened land degradation, water scarcity, and fluctuating agricultural productivity (Zhu et al., 2022; Faraslis et al., 2023; Abdelrahman & Arafat, 2020). In this context, robust agricultural land suitability assessment is essential for optimizing land use, enhancing crop yields, and supporting adaptive management strategies under changing environmental conditions (Choudhary et al., 2023; Anusah et al., 2023).

Traditional approaches to land evaluation have often relied on field surveys and expert judgment, which can be time-consuming and limited in spatial coverage. The integration of Geographic Information Systems (GIS) and Remote Sensing (RS) technologies has revolutionized spatial analysis by enabling the efficient collection, processing, and interpretation of large-scale environmental data (Mostafiz et al., 2021; Saha et al., 2019). These tools facilitate the extraction of critical biophysical indicators such as the Soil Moisture Index (SMI), Normalized Difference Vegetation Index (NDVI), Land Use/Land Cover (LULC), Land Surface Temperature (LST), and agro-physiographic parameters each playing a pivotal role in determining agricultural potential under variable climatic regimes (Saha et al., 2019; Donmez et al., 2024).

Multi-Criteria Decision Analysis (MCDA) frameworks have further enhanced land suitability modeling by systematically integrating diverse criteria into a unified decision-making process. Among MCDA techniques, the Analytical Hierarchy Process (AHP), particularly when employing the eigenvector method for weight derivation, stands out for its transparency, consistency checking, and ability to incorporate both quantitative data and expert knowledge (Saaty, 1980; Malczewski, 2004; Choudhary et al., 2023, Wijesinghe, 2024). The AHP's pairwise comparison matrix enables rigorous weighting of factors such as slope, elevation, distance from water bodies subcomponents that collectively define agro-physiographic suitability (Faraslis et al., 2023).

Model validation remains a critical step in spatial suitability analysis. The Area Under the Receiver Operating Characteristic Curve (AUC/ROC) approach is widely recognized for quantifying model predictive accuracy by comparing mapped suitability against observed outcomes or independent reference data. High AUC values (>0.80) reported in recent applications underscore the reliability of GIS-AHP frameworks for guiding land management decisions in complex environments (Shinde et al., 2024; Küçüker & Giraldo, 2022).

Despite methodological advances globally, there remains a notable research gap regarding comprehensive agricultural zoning using integrated GIS-RS-AHP approaches in North African contexts particularly within Algeria's Blida Wilaya. Existing studies often focus on broader Mediterranean or Middle Eastern settings or address adjacent applications such as groundwater or erosion risk mapping rather than direct agricultural suitability under current climate pressures (Chemirik et al., 2024; Mihi & Benaradj, 2022).

This study aims to address this gap by developing a high-resolution agricultural zoning model by using GIS-RS-derived indicators weighted via the AHP eigenvector method. By incorporating SMI, NDVI, LULC, LST, and an integrated Agro-physiographic parameter and validating results with AUC/ROC analysis the research seeks to provide actionable insights for sustainable land use planning in semi-arid Mediterranean landscapes.

Materials and Methods

Study Area

Blida Wilaya (wilaya code 09) is situated in the Tell region of northern Algeria, approximately 50 km south-west of Algiers and centered near 36°28′ N, 2°49′ E (Fig. 1). It extends over 1,480 km^2 and is bounded by the wilayas of Tipaza to the west, Algiers to the north, Boumerdès to the east, and Bouira, Médéa and Aïn Defla to the south and south-west.

Administratively, the wilaya comprises 25 municipalities and hosts more than one million inhabitants (1,002,937 at the 2008 General Population and Housing Census), corresponding to a density of nearly 678 inhabitants/km^2 among the highest in Algeria (ONS, 2008).

The territory is organized into three contrasting physiographic units that structure its agricultural geography (Fig. 1). The northern sector is occupied by the western part of the Mitidja plain, one of Algeria's most fertile alluvial basins (ca. 65 km in total length), whose deep Quaternary soils and extensive groundwater reservoir support intensive citrus, orchard, vegetable and cereal production (Bellout et al., 2020). Elevations below 150 m cover 39.14% of the wilaya, and gentle slopes (<5%) account for 37.24% of its surface, both concentrated in this unit. To the south, the plain rises abruptly into the Blidean Atlas, the easternmost calcareous massif of the Tell Atlas, whose summits exceed 1,500 m and of which roughly 2.9% of the wilaya lies above 1,200 m. This mountainous hinterland hosts the Chréa National Park (established 1985; ca. 26,000 ha), part of the UNESCO Chréa Biosphere Reserve, renowned for its Atlas cedar (Cedrus atlantica), holm oak and Aleppo pine stands and for the Barbary macaque (Macaca Sylvanus) populations (UNESCO-MAB, 2025). Between the two lies a piedmont corridor of plains and foothills along which the largest urban centres (Blida, Ouled Yaïch, Beni Mered, Boufarik, Larbaa and Meftah) have coalesced, exposing some of the wilaya's best alluvial soils to rapid peri-urban expansion.

The wilaya experiences a Mediterranean climate (Köppen Csa) of semi-arid to sub-humid character, with hot, dry summers and mild, wet winters. Mean annual precipitation is approximately 640 mm at plain stations and increases to more than 800 mm in the Atlas massif, as documented in the Chiffa basin (Madani et al., 2024), whereas the mean annual temperature is close to 17°C at Blida station. Rainfall is strongly concentrated between November and March, and the pronounced summer water deficit constitutes the principal climatic constraint on rainfed agriculture, underpinning the importance of soil moisture as a suitability criterion. The hydrographic network drains the mountain front and crosses the plain: Oued Chiffa, incised in the eponymous gorges, joins Oued Mazafran along the western boundary before reaching the sea; Oued Bou Roumi is impounded by the Bou Roumi dam for irrigation and water supply; Oued Djer drains the south-western margin towards the Chelif basin; and the eastern plain is drained towards the Algiers region by Oued El Harrach. This juxtaposition of a highly productive irrigated plain, a conserved forested mountain belt and an expanding urban corridor, under seasonal water stress, renders Blida Wilaya a representative case for agricultural potential mapping in semi-arid Mediterranean landscapes.

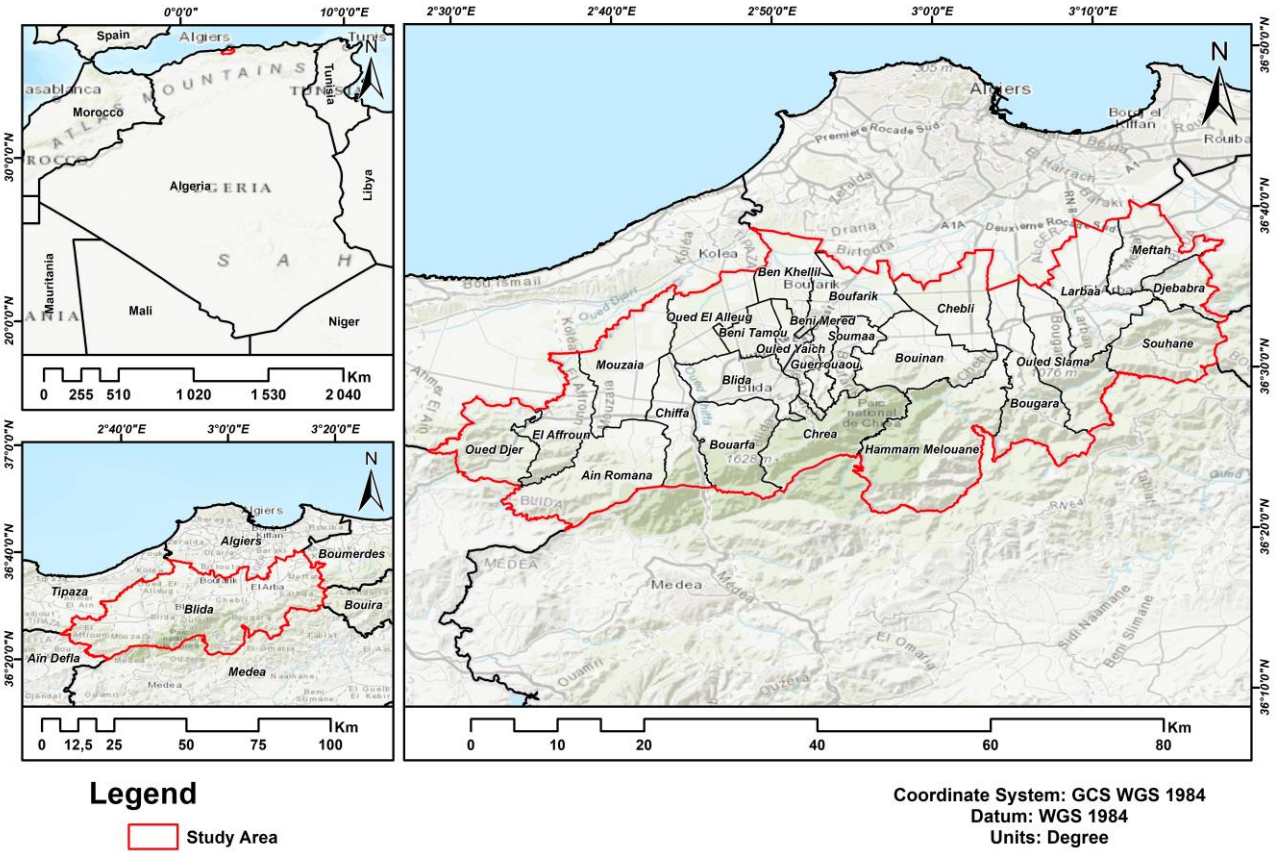


Fig. 1: Geographic Location of Wilaya of Blida.

Data Collection

A comprehensive geospatial database was assembled from multi-source remote sensing imagery and open-access geographic datasets (Fig. 2). The primary optical dataset consisted of Landsat 8 Operational Land Imager (OLI) and Thermal Infrared Sensor (TIRS) scenes acquired during the 2025 growing season, selected for minimal cloud contamination (<5%) and a spatial resolution of 30 m (USGS, 2025). Topographic parameters (slope and elevation) were derived from the Shuttle Radar Topography Mission Digital Elevation Model (SRTM DEM) at 30 m resolution. Hydrographic features (rivers, wadis, dams, and lakes) were extracted from the OpenStreetMap (OSM) dataset and clipped to the administrative boundary of the study area. All raster layers were reprojected to the Universal Transverse Mercator (UTM) Zone 31N coordinate reference system and resampled to a uniform 30 × 30 m pixel grid to ensure spatial interoperability across the analytical workflow.

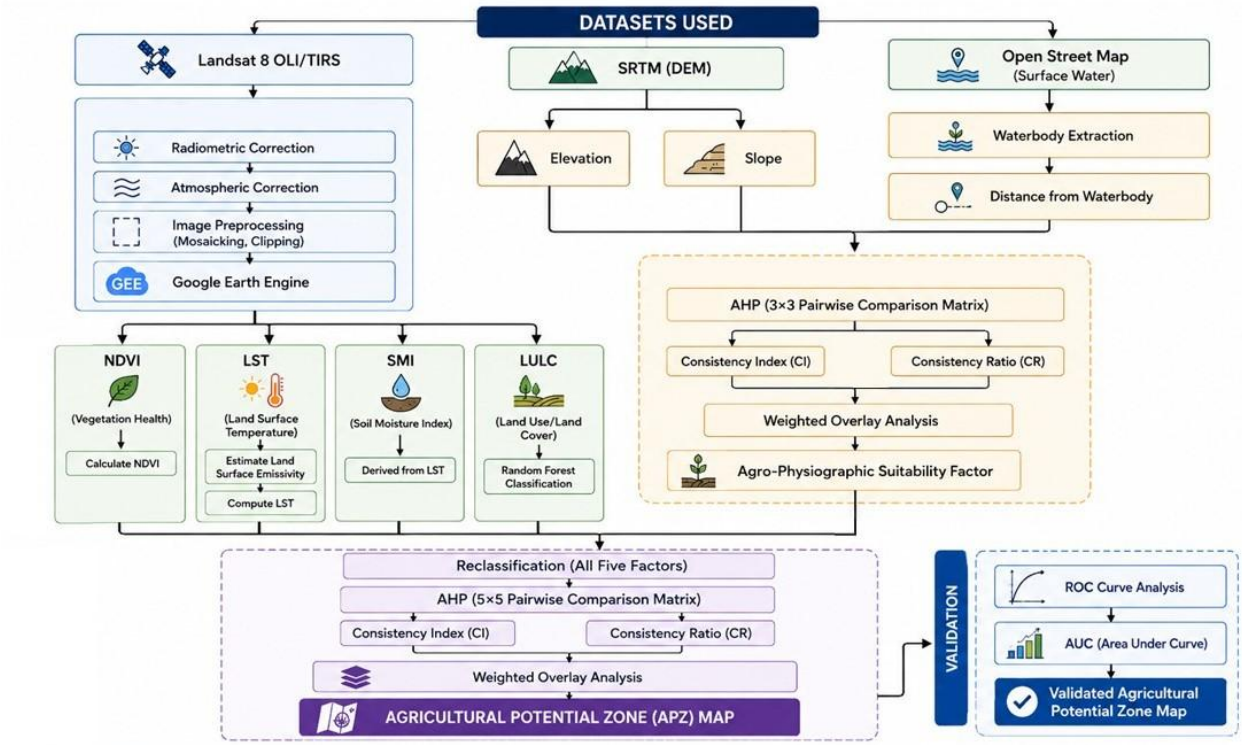


Fig. 2: General flowchart of study methodology.

Preprocessing of satellite imagery (including atmospheric correction, radiometric calibration, and geometric verification) was performed within the Google Earth Engine (GEE) cloud-based platform. Subsequent raster reclassification, vector overlay operations, and cartographic composition were executed in ArcGIS 10.8 (ESRI, 2016).

Preparation of Thematic Layers

Five spatial criteria governing agricultural potential were extracted and prepared as individual raster layers prior to their integration within the multi-criteria decision framework.

- **Normalized Difference Vegetation Index (NDVI):** Vegetation vigor and photosynthetic activity were quantified using the classical NDVI formulation (Cetin et al., 2022):

$$NDVI = \frac{\rho_{NIR} - \rho_{RED}}{\rho_{NIR} + \rho_{RED}}$$

where ρ_{NIR} and ρ_{RED} denote the surface reflectance values in the near-infrared (Band 5) and red (Band 4) spectral channels, respectively.

- **Land Surface Temperature (LST):** LST retrieval followed the single-channel radiative transfer algorithm adapted for Landsat 8 TIRS bands (Jesus & Santana, 2017, Machireddy, 2025). The procedure involved three sequential steps. First, the Proportion Vegetation (P_V) was estimated from the NDVI:

$$P_V = \left(\frac{NDVI - NDVI_{min}}{NDVI_{max} - NDVI_{min}}\right)^2$$

Second, the land surface emissivity (ε_λ) was computed as:

$$\varepsilon_\lambda = 0.004 \times P_V + 0.986$$

Third, the at-sensor spectral radiance of thermal Band 10 was calculated as:

$$L_\lambda = M_L \times Q_{CAL} + A_L$$

where M_L is the band-specific multiplicative rescaling factor and A_L the additive rescaling factor, both extracted from the image metadata. The brightness temperature (BT) was subsequently derived via the inverse Planck function:

$$BT = \frac{K_2}{\ln\left(\frac{K_1}{L_\lambda} + 1\right)} - 273.15$$

where K_1 and K_2 are band-specific thermal conversion constants. The final LST was obtained through emissivity correction:

$$LST = \frac{BT}{1 + \left(\frac{\lambda \times BT}{\rho}\right) \times \ln \varepsilon_\lambda}$$

where λ is the effective wavelength of Band 10 (10.9 μm) and $\rho = hc/\sigma = 1.438 \times 10^{-2}$m·K, with $h$representing Planck's constant, c the speed of light, and σ the Boltzmann constant.

- **Soil Moisture Index (SMI).** The SMI was derived from the normalized LST approach, exploiting the inverse relationship between surface thermal emission and root-zone water content (Machireddy, 2025):

$$SMI = \frac{LST_{max} - LST}{LST_{max} - LST_{min}}$$

where LST_{min} and LST_{max} correspond to the extreme thermal values within the scene. This index provides a spatially continuous proxy of soil hydrological status directly relevant to crop water availability.

- **Land Use/Land Cover (LULC).** A supervised classification was performed using the Random Forest algorithm within the GEE environment. The classifier was trained on spectrally homogeneous reference polygons and yielded seven land-cover categories: water bodies, built-up areas, bare areas, shrubland, forest, grassland, and cropland. Post classification accuracy assessment and majority filter smoothing were applied to reduce salt and pepper noise.
- **Agro-Physiographic Suitability.** A composite terrain index was constructed by integrating three sub criteria (slope, elevation, and distance from water bodies) through a dedicated three-factor AHP (Fig 2). Slope and elevation were extracted from the SRTM DEM using standard GIS terrain analysis algorithms. Distance from water bodies was computed via Euclidean distance allocation from the vectorized hydrographic network. The resulting continuous surface was reclassified into five ordinal suitability zones.

Agricultural Potential Mapping Method

Analytic Hierarchy Process

The integration of the five thematic layers into a unified agricultural potential map was achieved through the Analytic Hierarchy Process (AHP), a structured multi-criteria decision analysis (MCDA) technique originally formalized by Saaty (1980). The AHP decomposes a complex spatial decision problem into a hierarchical structure of criteria and sub-criteria, enabling the systematic quantification of relative factor importance through pairwise comparisons.

Pairwise Comparison Matrix Construction

Two levels of pairwise comparison matrices were constructed. At the sub-criterion level, a 3 × 3 reciprocal matrix (Fig. 3) was assembled for the Agro-Physiographic factor (slope, elevation, and distance from water bodies) using Saaty's (1980) fundamental 1-9 scale of relative importance (Tab. 1). At the criterion level, a 5 × 5 matrix (Fig. 4) was built for the five principal factors (SMI, NDVI, Agro-Physiographic Suitability, LULC, and LST). Judgments were grounded in the agronomic and biophysical literature concerning Mediterranean semi-arid landscapes (Faraslis et al., 2023; Zhu et al., 2022). Soil moisture was assigned to have the highest dominance owing to its immediate control on plant-water availability, while LST received the lowest comparative weight given its more indirect thermal regulation role. The matrices satisfy the conditions of diagonal unity ($a_{ii} = 1$) and reciprocity ($a_{ji} = 1/a_{ij}$).

Tab. 1: Saaty's Fundamental Scale of Relative Importance (Saaty, 1980)

Score	Verbal Judgement	Explanation
1	Equal importance	Two criteria contribute equally to the objective

2	Weak or slight	
3	Moderate importance	Experience and judgement slightly favour one over another
4	Moderate plus	
5	Strong importance	Experience and judgement strongly favour one over another
6	Strong plus	
7	Very strong importance	A criterion is favoured very strongly; its dominance is demonstrated in practice
8	Very, very strong	
9	Extreme importance	The evidence favouring one over another is of the highest possible order

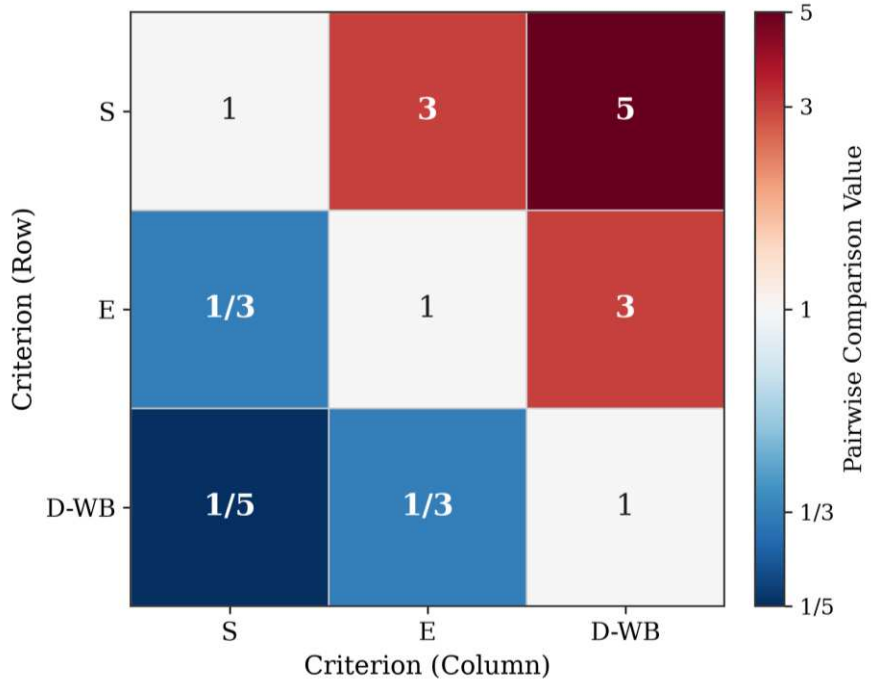


Fig. 3: Agro-Physiographic Suitability AHP Pairwise Comparison Matrix (Note: S=Slope, E=Elevation, D-WB=Distance from Waterbody).

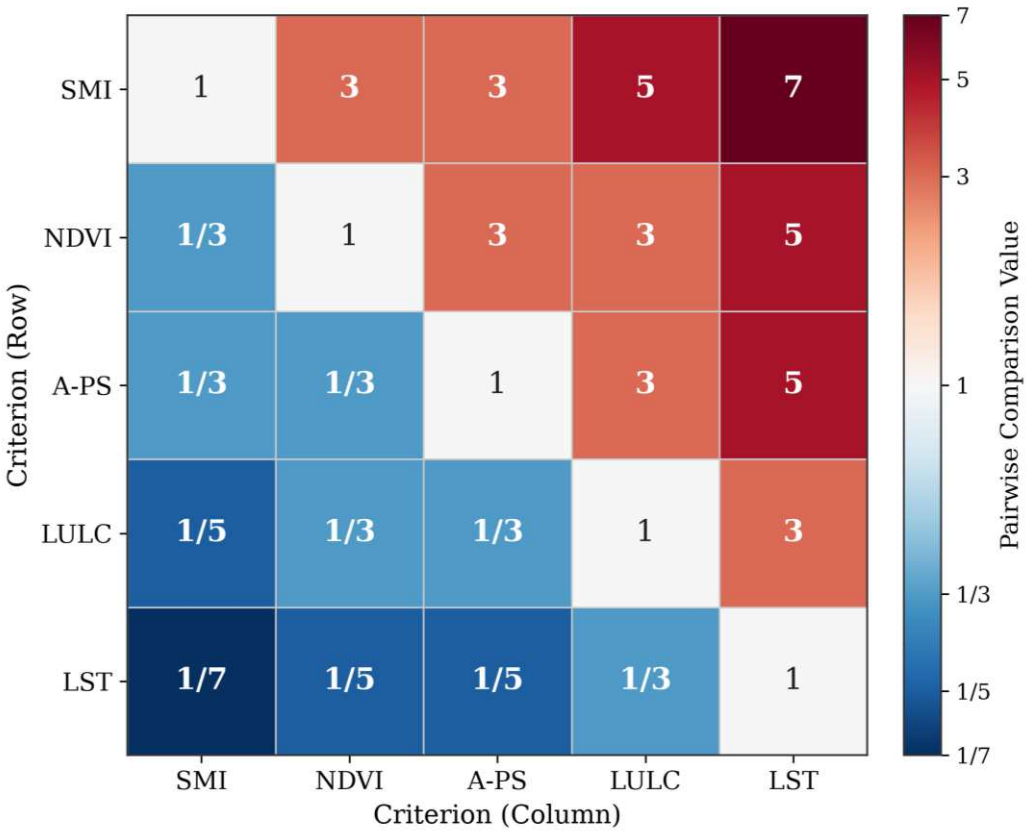


Fig. 4: Agricultural Potential Zones AHP Pairwise Comparison Matrix (Note: SMI=Soil Moisture Index, NDVI=Normalized Difference Vegetation Index, A-PS= Agro-Physiographic Suitability, LULC=Land Use Land Cover, LST=Land Surface Temperature).

Priority Vector (Eigenvector Method)

Relative weights were computed following Saaty's principal right eigenvector method (Saaty, 1977, 2003). The procedure comprised two operations. First, each column of the pairwise comparison matrix was normalized by dividing every element by its respective column sum, yielding the normalized matrix $\bar{A}$. Second, the priority vector $\boldsymbol{w}$ was obtained by averaging the rows of $\bar{A}$:

$$w_i = \frac{1}{n}\sum_{j=1}^{n} \bar{a}_{ij}$$

By construction, $\sum_{i=1}^{n} w_i = 1$, ensuring that weights represent proportional contributions to total criterion importance (Escobar et al., 2004; Klein, 2019). For the five-factor matrix, the derived weights were:

SMI = 0.4502, NDVI = 0.2502, Agro-Physiographic Suitability = 0.1697, LULC = 0.0872, and LST = 0.0427 (Tab. 3).

For the three-factor Agro-Physiographic sub-matrix, the weights were: Slope = 0.6333, Elevation = 0.2605, and Distance from Waterbody = 0.1062 (Tab. 2).

Consistency Assessment

The internal logical coherence of pairwise judgments was verified through the Consistency Ratio (CR) (Saaty, 1987). The maximum eigenvalue (λ_{max}) was estimated as:

$$\lambda_{max} = \frac{1}{n}\sum_{i=1}^{n} \frac{(A \cdot w)_i}{w_i}$$

The Consistency Index (CI) was then calculated:

$$CI = \frac{\lambda_{max} - n}{n - 1}$$

and normalized against the Random Index (RI) corresponding to the matrix dimension:

$$CR = \frac{CI}{RI}$$

For the five-factor matrix ($n = 5$, $RI = 1.12$), the computed values were $\lambda_{max} = 5.28$, $CI = 0.070$, and $CR = 6.25\%$.

For the three-factor sub-matrix ($n = 3$, $RI = 0.58$), $\lambda_{max} = 3.04$, $CI = 0.019$, and $CR = 3.34\%$. Both ratios fall well below the 10% acceptability threshold (Saaty, 1980), confirming that the elicited judgments are logically consistent and that the derived weight vectors are reliable for spatial aggregation.

Spatial Aggregation and Reclassification

The final Agricultural Potential Zone map was generated through weighted linear combination (WLC) of the five reclassified raster layers, each multiplied by its respective AHP-derived weight. The continuous suitability score was subsequently segmented into five ordinal classes: Not Suitable for Agriculture, Marginally Suitable, Moderately Suitable, Suitable for Agriculture, and Highly Suitable for Agriculture. The same five-class reclassification scheme was applied to each individual thematic layer to ensure uniformity in the interpretation of suitability gradients across the study area.

Validation

Model validation was performed using the Area Under the Receiver Operating Characteristic Curve (AUC/ROC), a widely applied method for assessing the predictive accuracy of spatial suitability models. The ROC curve describes the trade-off between true positive and false positive rates across classification thresholds, while the AUC quantifies the model's ability to discriminate between suitability classes. Higher AUC values indicate stronger predictive performance and greater reliability of the agricultural potential map (Shinde et al., 2024).

Results and Discussion

Suitability Analysis of Reclassified Factors

Slope

Slope governs the intensity of surface runoff, the rate of soil erosion, and the ease of agricultural mechanization, all of which directly condition land workability and moisture retention capacity. Gentle slopes favor water infiltration and reduce erosion hazards, thereby enhancing agricultural suitability, whereas steep slopes accelerate runoff, intensify soil loss, and constrain the use of farm machinery. Within the Agro-Physiographic AHP pairwise comparison matrix, slope received the highest normalized weight among the three topographic sub-criteria (Wi = 63.33%), reflecting its dominant control over the composite Agro-Physiographic Suitability factor. The reclassification of the slope map yielded five classes (Fig. 5): (1) slopes below 5% (37.24% of the study area), assigned Very High suitability owing to their near-flat topography favorable for cultivation and irrigation; (2) slopes of 5–15% (14.54%), rated High; (3) slopes of 15–30% (23.99%), rated Medium; (4) slopes of 30–50% (21.29%), rated Low due to increasing erosion susceptibility; and (5) slopes exceeding 50% (2.94%), rated Very Low, corresponding to the steep, erosion-prone terrain least suited to agricultural use.

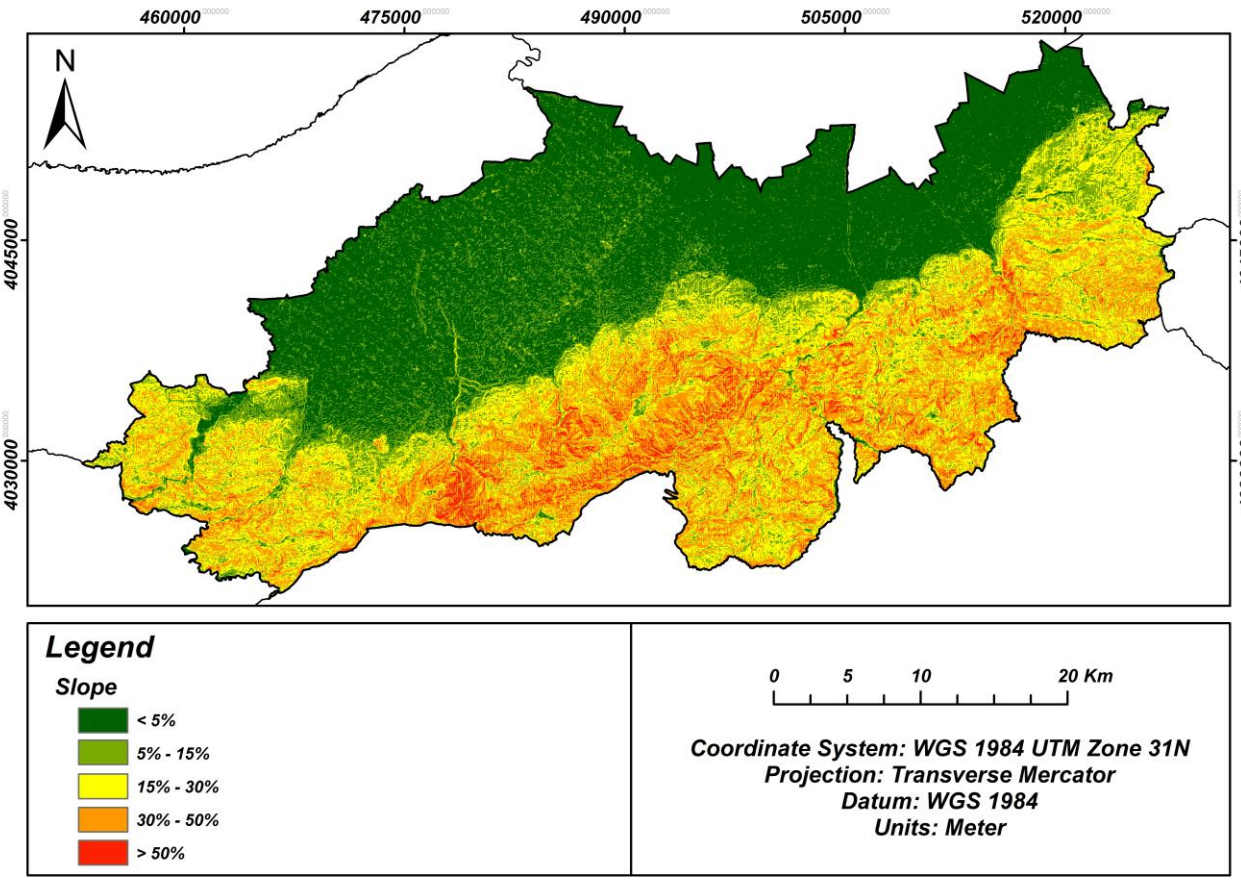


Fig. 5: Slope Map.

Elevation

Elevation exerts an indirect but significant influence on agricultural potential through its control over local thermal regimes, precipitation gradients, soil depth accumulation, and accessibility to farming infrastructure. Lower elevations in the study area generally coincide with deeper alluvial soils, milder temperatures, and easier access for irrigation and equipment, while higher elevations impose thermal limitations and thinner, less developed soils that reduce cultivable potential. Elevation was assigned a normalized weight of 26.05% within the Agro-Physiographic AHP matrix, the second most influential topographic criterion after slope. The reclassified elevation map comprises five classes (Fig. 6): (1) below 150 m (39.14%), rated Very High; (2) 150–300 m (13.42%), rated High; (3) 300–600 m (20.57%), rated Medium; (4) 600–1,200 m (23.95%), rated Low; and (5) above 1,200 m (2.92%), rated Very Low, representing the mountainous fringes of the wilaya where agricultural activity is markedly constrained.

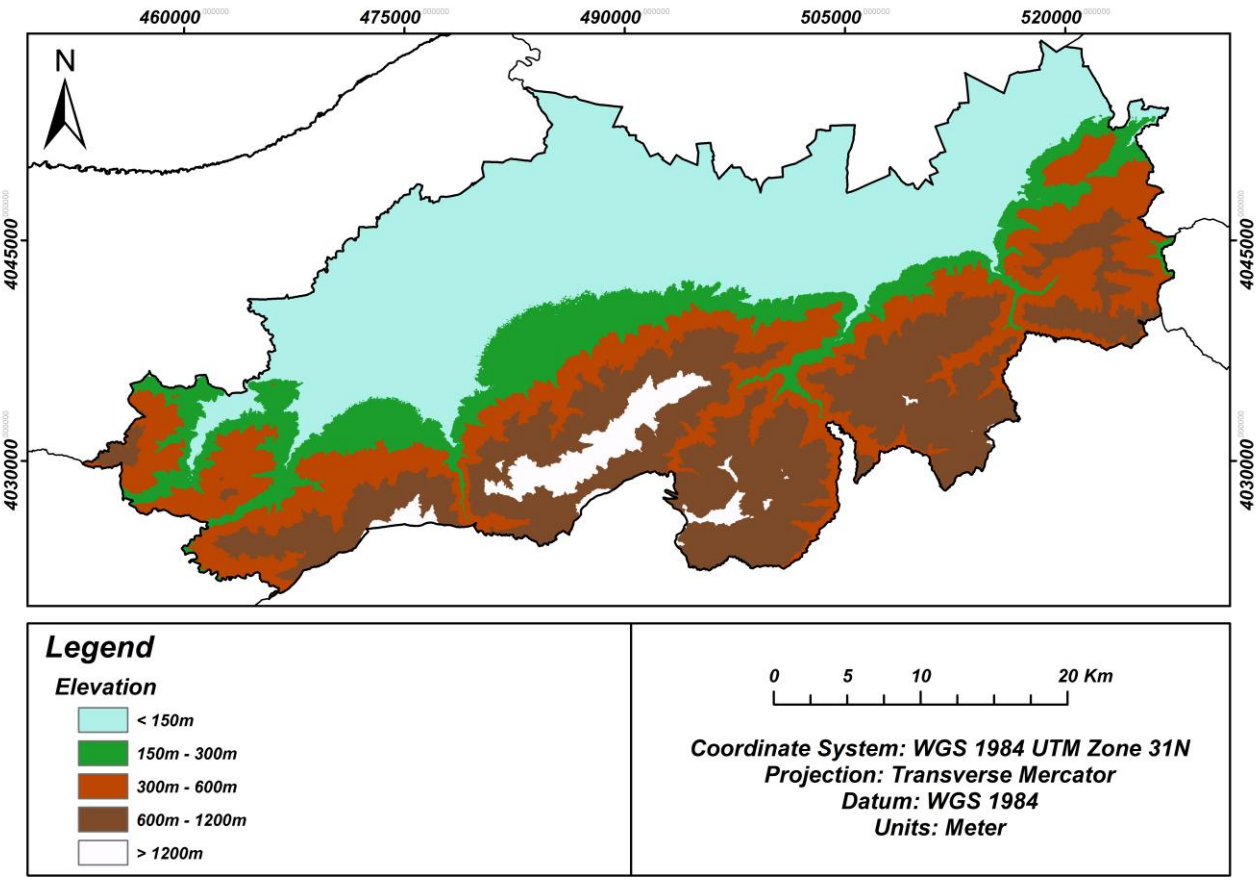


Fig. 6: Elevation Map.

Distance from Waterbody

Proximity to surface water bodies (rivers, wadis, and reservoirs) determines the accessibility of irrigation water, sustains near-channel soil moisture through lateral seepage, and supports local groundwater recharge factors that are particularly critical for agricultural productivity under the semi-arid Mediterranean climate of Blida. Parcels located close to watercourses benefit from a more reliable water supply and reduced drought risk, whereas distant parcels depend primarily on rainfed conditions and are more exposed to water stress. Distance from Waterbody carried the lowest weight among the three Agro-Physiographic sub-criteria (Wi = 10.62%), reflecting its comparatively secondary, though still relevant, role relative to slope and elevation. The reclassification produced five buffer-based classes (Fig. 7): (1) less than 500 m (7.66%), rated Very High; (2) 500–1,000 m (6.86%), rated High; (3) 1,000–2,000 m (13.92%), rated Medium; (4) 2,000–5,000 m (35.18%), rated Low; and (5) beyond 5,000 m (36.39%), rated Very Low, this last class covering the largest share of the study area and underscoring the limited surface-water accessibility across much of the wilaya.

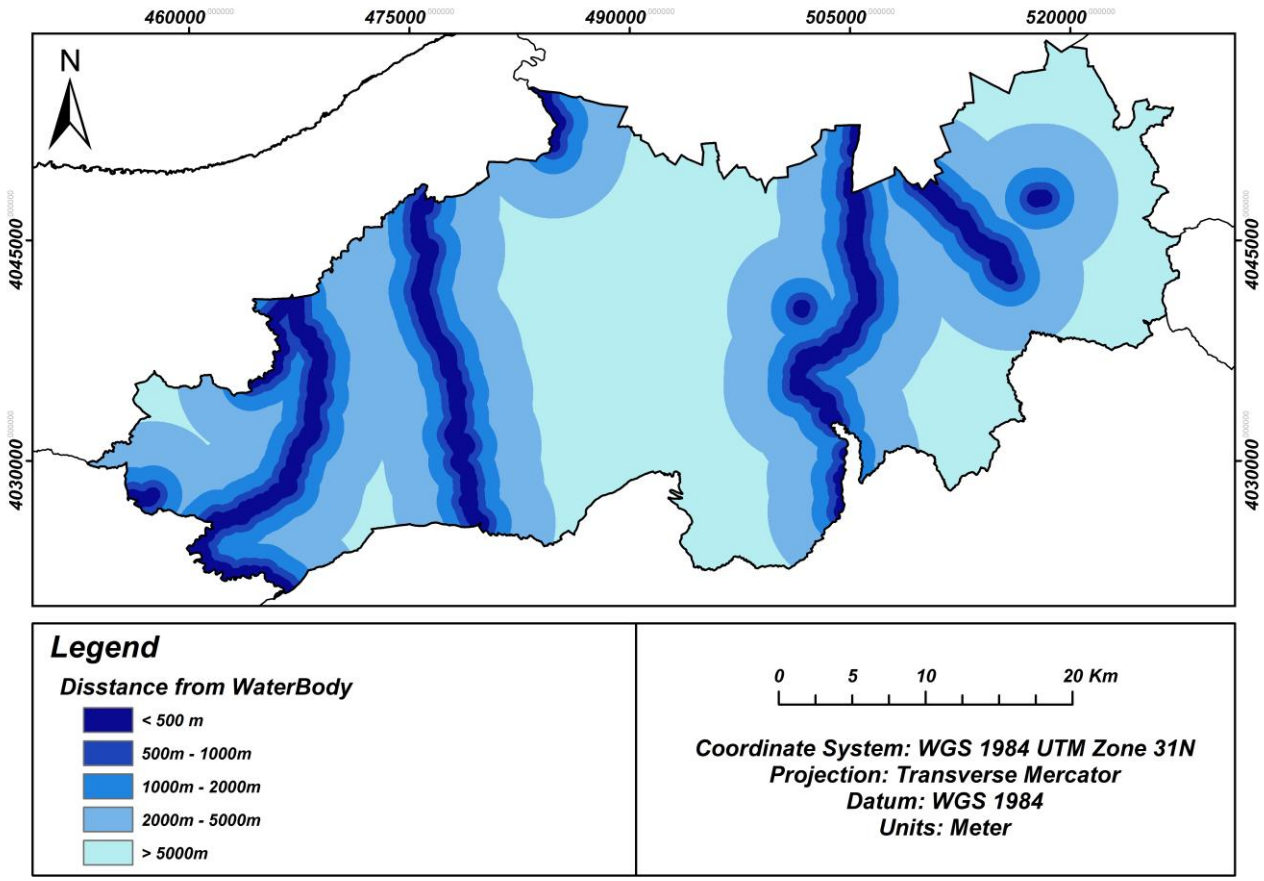


Fig. 7: Distance from Waterbody Map.

Agro-Physiographic Suitability

The Agro-Physiographic Suitability factor is a composite index derived from the integration of slope, elevation, and distance from waterbody. Rather than describing a single biophysical process, this factor synthesizes the terrain's inherent physical capacity to sustain agriculture, independent of dynamic vegetative or thermal conditions and was subsequently reintroduced as a single input within the final five-factor AHP model, where it received a normalized weight of 16.97%. Its reclassified output delineates five suitability zones across the study area (Fig. 8): (1) an Unfavorable Agro-Physiographic Zone (3.87%), corresponding to areas of steep slope, high elevation, and/or remoteness from water sources; (2) a Marginally Favorable Zone (24.98%); (3) a Moderately Favorable Zone (20.36%); (4) a Favorable Agro-Physiographic Zone (12.75%); and (5) a Highly Favorable Agro-Physiographic Zone (38.05%), which occupies the largest proportion of the wilaya and reflects the generally low-relief, water-accessible character of the Metija plain.

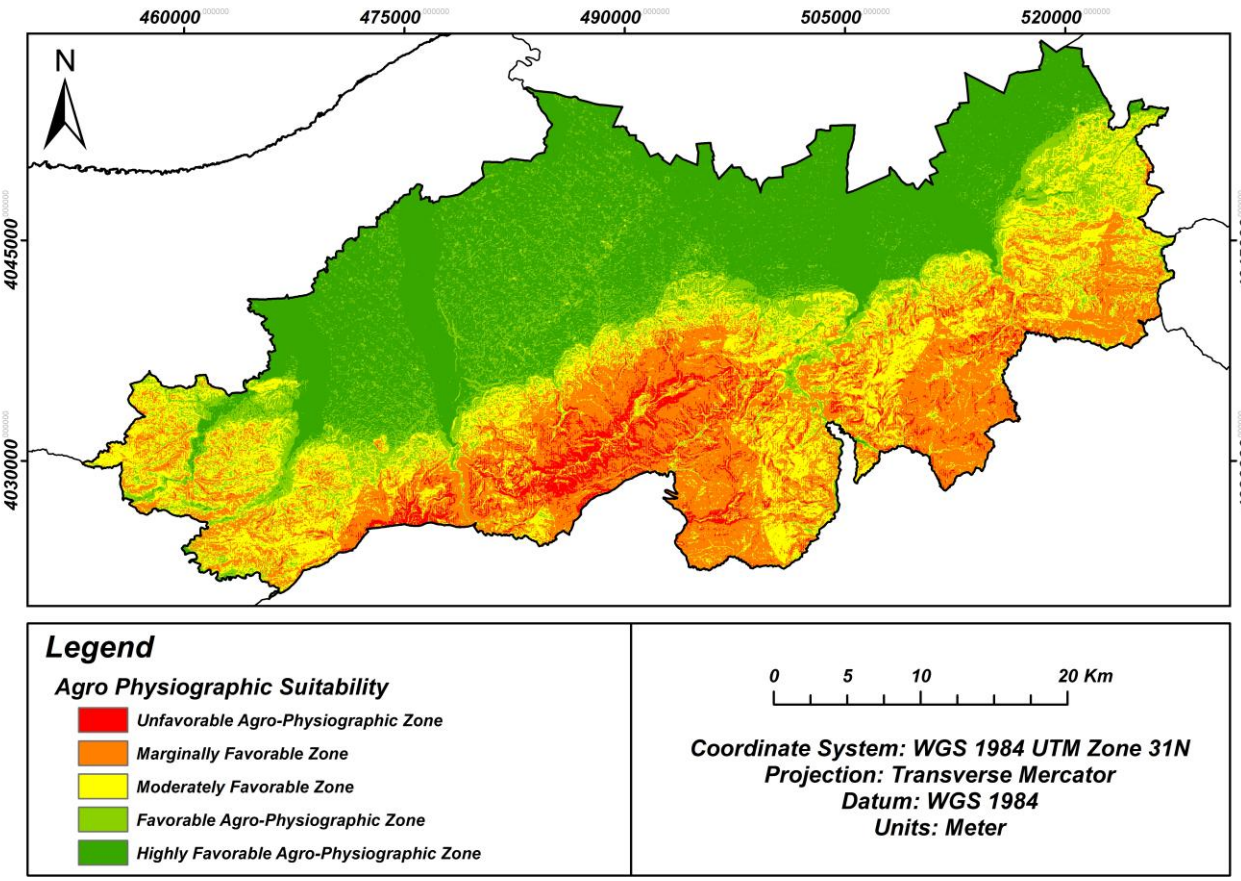


Fig. 8: Agro-Physiographic Suitability Map.

Soil Moisture Index (SMI)

The Soil Moisture Index reflects the water content available within the root zone and constitutes a key determinant of seed germination, plant water stress, and overall drought vulnerability, particularly under the semi-arid rainfed conditions that characterize much of the study area. SMI captures short-term soil hydrological status directly relevant to crop establishment and yield potential. Owing to its strong and immediate influence on plant-available water, SMI was assigned the highest weight among the five factors in the final AHP matrix (Wi = 45.02%). The reclassified SMI map is divided into five moisture classes (Fig. 9): (1) 0–0.2, denoting Very Dry Soil (0.97%) and rated Very Low; (2) 0.2–0.4, Dry Soil (49.22%), rated Low and covering nearly half of the study area; (3) 0.4–0.6, Moderately Moist Soil (41.98%), rated Medium; (4) 0.6–0.8, Moist Soil (7.82%), rated High; and (5) 0.8–1, Saturated / Very Moist Soil (0.005%), rated Very High but occupying a negligible share of the wilaya, largely confined to permanently wet or irrigated patches.

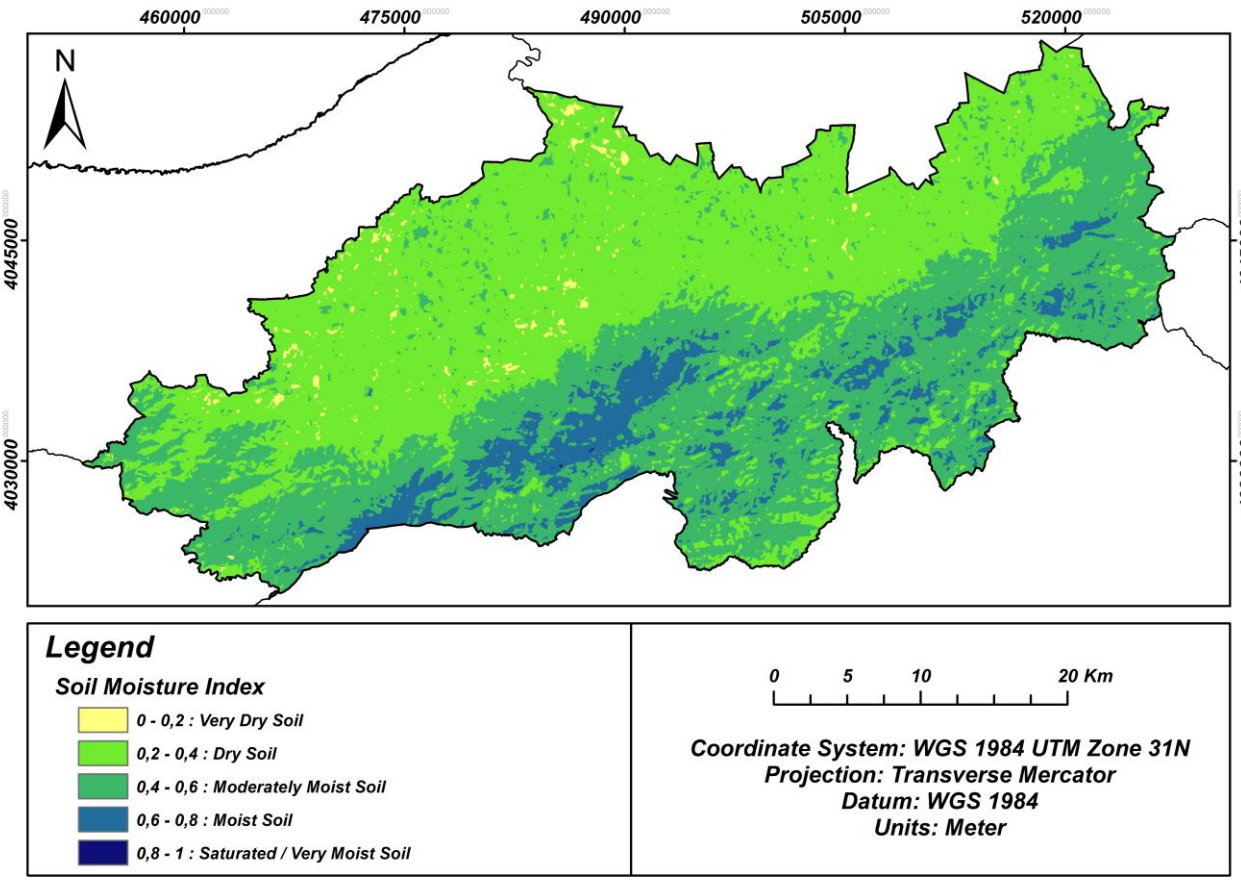


Fig. 9: Soil Moisture Index Map.

Normalized Difference Vegetation Index (NDVI)

NDVI quantifies vegetation vigor and green biomass density from the contrast between red and near-infrared reflectance and serves as a proxy for current photosynthetic activity and land productivity. Zones of dense, healthy vegetation cover indicate high existing biological productivity favorable to agriculture, whereas negative or near-zero values correspond to open water, bare soil, or degraded surfaces unsuitable for cropping. NDVI was assigned the second-highest weight in the final AHP matrix (Wi = 25.02%), underscoring its importance as a direct indicator of vegetative health. The reclassification yielded five vegetation classes (Fig. 10): (1) values below 0, classified as Water (0.07%) and rated Very Low; (2) 0–0.2, Bare Soil (4.77%), rated Low; (3) 0.2–0.4, Sparse Vegetation (16.20%), rated Medium; (4) 0.4–0.6, Moderate Vegetation (37.19%), rated High; and (5) values above 0.6, Dense Vegetation (41.76%), rated Very High and representing the largest share of the wilaya, consistent with the extensive cropland and forest cover of the region.

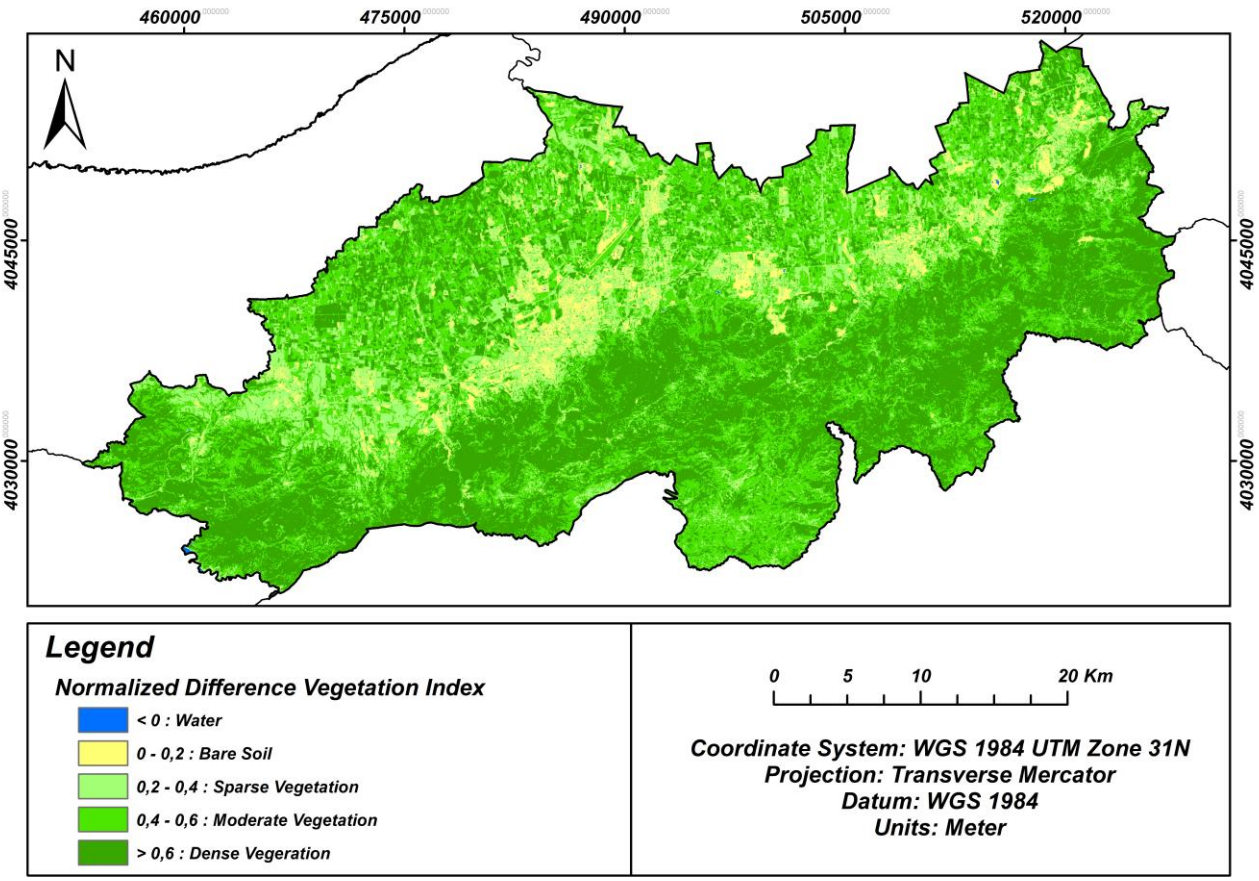


Fig. 10: Normalized Difference Vegetation Index Map.

Land Use / Land Cover (LULC)

LULC identifies the actual current use and cover of the land and is essential for distinguishing areas already under active cultivation from those structurally unavailable for agriculture (built-up areas, water bodies) or requiring land-cover conversion (shrubland, bare ground). Unlike the continuous biophysical indices, LULC suitability was assigned according to the land-use category itself rather than a numerical gradient. Seven classes were identified (Fig. 11): (1) Water Body (0.05%), rated Very Low; (2) Build Up (9.40%), rated Very Low, reflecting urbanized land unavailable for cultivation; (3) Bare areas (0.02%), rated Low; (4) Shrubland (10.17%), rated Medium; (5) Forest (45.01%), also rated Medium and comprising the single largest land-cover class in the wilaya; (6) Grassland (0.42%), rated High; and (7) Cropland (34.94%), rated Very High, representing land already under active agricultural exploitation. LULC was assigned a normalized weight of 8.72% within the final AHP matrix.

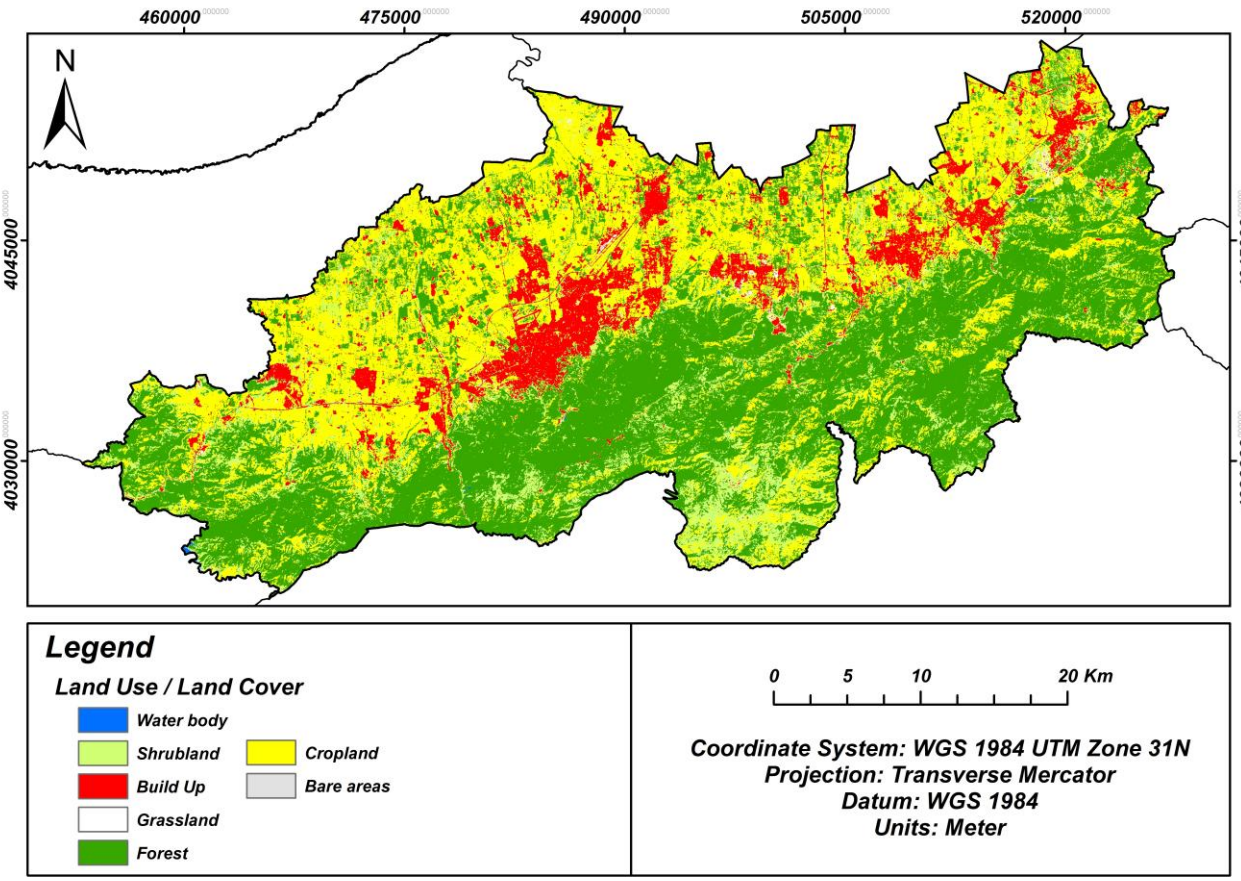


Fig. 11: Land Use/ Land Cover Map.

Land Surface Temperature (LST)

Land Surface Temperature governs evapotranspiration rates and crop heat stress and also served as the basis for deriving the Soil Moisture Index. Moderate-to-warm surface temperatures generally favor photosynthetic activity and crop development, whereas extreme heat suppresses metabolic processes, increases crop water demand, and elevates the risk of moisture deficit. LST received the lowest weight among the five factors in the final AHP matrix (Wi = 4.27%), reflecting its comparatively indirect, though non-negligible, influence relative to the vegetative and moisture-based indicators. The reclassified LST map comprises five thermal classes (Fig. 12): (1) below 25°C, Moderate Surface Temperature (2.64%), rated Medium; (2) 25–30°C, Warm Surface Temperature (19.30%), rated Very High and the most favorable thermal range for crop growth; (3) 30–35°C, Hot Surface Temperature (30.39%), rated High; (4) 35–40°C, Very Hot Surface Temperature (41.69%), rated Low, covering the largest share of the wilaya; and (5) above 40°C, Extremely Hot Surface Temperature (5.99%), rated Very Low, corresponding to the most thermally stressed surfaces least conducive to agricultural productivity.

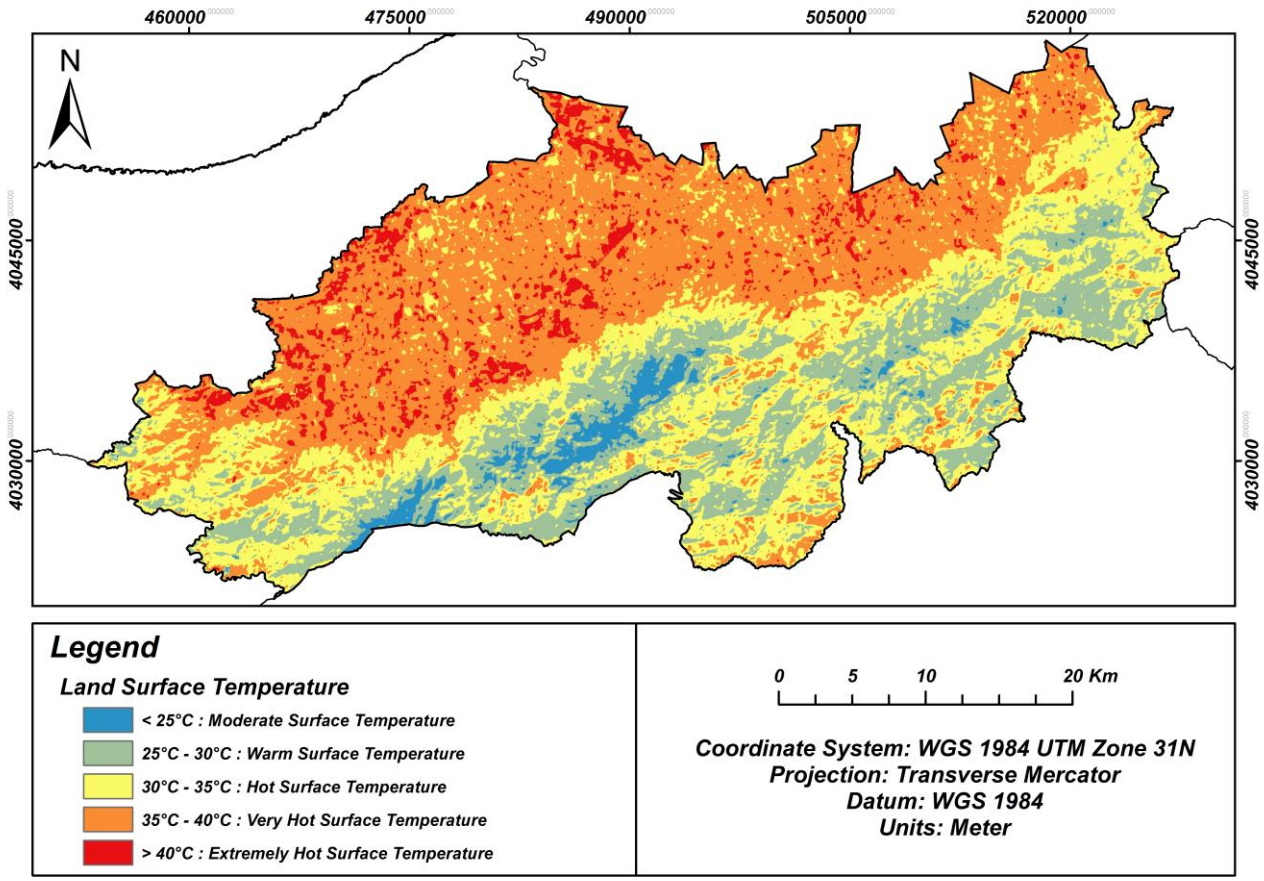


Fig. 12: Land Surface Temperature Map.

AHP-Derived Weights of the Suitability Factors and Their Classes

Tab. 2: Assigned weight and normalized weights of respective classes of factors influencing Agro-Physiographic Suitability.

Factor	Factor's Normalized Weights Wi (%)	Classes	Assigned weight	Influence on Agro-Physiographic Suitability Map	Area (ha)	Area (%)
Slope	**63,33%**	< 5%	5	Very High	55137,23	37,24%
		5% - 15%	4	High	21524,32	14,54%
		15% - 30%	3	Medium	35520,19	23,99%
		30% - 50%	2	Low	31517,46	21,29%
		> 50%	1	Very Low	4347,24	2,94%
Elevation	**26,05%**	< 150m	5	Very High	57951,88	39,14%
		150m - 300m	4	High	19866,05	13,42%
		300m - 600m	3	Medium	30449,00	20,57%
		600m - 1200m	2	Low	35461,12	23,95%
		> 1200m	1	Very Low	4318,37	2,92%
Distance from Waterbody	**10,62%**	< 500m	5	Very High	11337,69	7,66%
		500m - 1000m	4	High	10153,02	6,86%
		1000m - 2000m	3	Medium	20603,77	13,92%

		2000m - 5000m	2	Low	52075,77	35,18%
		> 5000m	1	Very Low	53876,17	36,39%

343

344 ***Tab. 3: Assigned weight and normalized weights of respective classes of factors influencing Agriculture Potential***

345 ***Zones.***

Factor	Factor's Normalized Weights Wi (%)	Classes	Assigned weight	Influence on Agriculture Potential Zones	Area (ha)	Area (%)
Soil Moisture Index (SMI)	**45,02%**	0 - 0,2 : Very Dry Soil	1	Very Low	1439,16	0,97%
		0,2 - 0,4 : Dry Soil	2	Low	72870,52	49,22%
		0,4 - 0,6 : Moderately Moist Soil	3	Medium	62152,11	41,98%
		0,6 - 0,8 : Moist Soil	4	High	11577,38	7,82%
		0,8 - 1 : Saturated / Very Moist Soil	5	Very High	7,40	0,01%
Normalized Difference Vegetation Index (NDVI)	**25,02%**	< 0 : Water	1	Very Low	105,71	0,07%
		0 - 0,2 : Bare Soil	2	Low	7066,70	4,77%
		0,2 - 0,4 : Sparse Vegetation	3	Medium	23989,89	16,20%
		0,4 - 0,6 : Moderate Vegetation	4	High	55059,21	37,19%
		> 0,6 : Dense Vegeration	5	Very High	61824,93	41,76%
Agro Physiographic Suitability	**16,97%**	Unfavorable Agro-Physiographic Zone	1	Very Low	5722,14	3,87%
		Marginally Favorable Zone	2	Low	36979,18	24,98%
		Moderately Favorable Zone	3	Medium	30143,58	20,36%
		Favorable Agro-Physiographic Zone	4	High	18872,37	12,75%
		Highly Favorable Agro-Physiographic Zone	5	Very High	56329,15	38,05%
Land Use / Land Cover (LULC)	**8,72%**	Water Body	1	Very Low	71,65	0,05%
		Shurbland	3	Medium	15053,95	10,17%
		Build Up	1	Very Low	13912,37	9,40%
		Grassland	4	High	620,76	0,42%
		Forest	3	Medium	66629,92	45,01%
		Cropland	5	Very High	51732,31	34,94%
		Bare areas	2	Low	25,32	0,02%
Land Surface Temperature (LST)	**4,27%**	< 25°C : Moderate Surface Temperature	3	Medium	3902,65	2,64%
		25°C - 30°C : Warm Surface Temperature	5	Very High	28567,48	19,30%
		30°C - 35°C : Hot Surface Temperature	4	High	44987,31	30,39%
		35°C - 40°C : Very Hot Surface Temperature	2	Very Low	61722,18	41,69%
		> 40°C : Extremely Hot Surface Temperature	1	Low	8866,80	5,99%

346

347 ***Validation***

348 The ROC curve was used to evaluate the predictive performance of the agricultural potential map derived using
349 the AHP method. The area under the curve (AUC) reached 0.93 (Fig. 13), indicating excellent discriminatory performance
350 of the model. This high AUC value suggests that the AHP-based approach effectively distinguishes areas with different
351 levels of agricultural potential. Overall, the results provide strong evidence of the model's predictive capability and
352 support the reliability of the generated agricultural potential map.

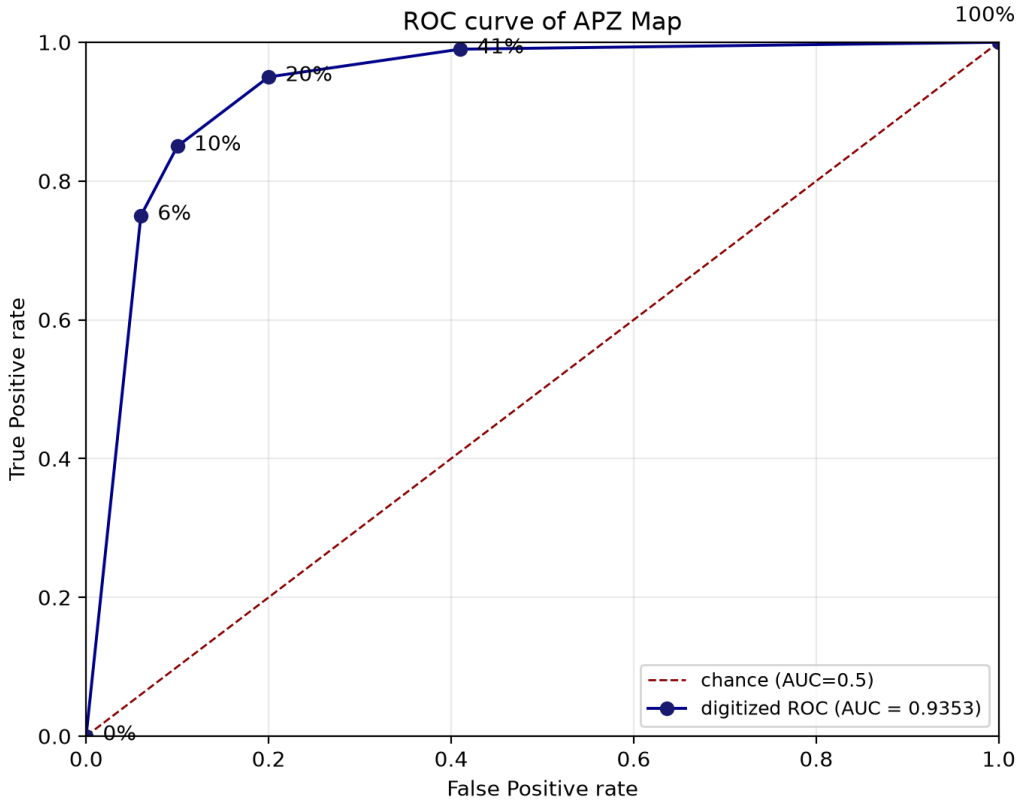


Fig. 13: Validation of APZ Map by ROC curve.

Discussion

Spatial structure of the mapped agricultural potential

The final APZ map (Fig. 14) organizes the wilaya into three legible bands. Red, not-suitable pixels cluster along the piedmont corridor that links Blida, Ouled Yaïch, Beni Mered, Boufarik, Larbaa and Meftah, and within the cores of the smaller towns; a dark-green, highly suitable belt runs south-west to north-east along the front of the Blidean Atlas, through Chréa, Hammam Melouane and Bougara, and reappears on the eastern hills of Djebabra and Souhane; between the two, a light-green suitable matrix covers the Mitidja plain and the broad intramontane valleys. At wilaya scale the suitable class dominates (70,179 ha; 47.40 % of 148,046 ha), followed by the moderately (33,351 ha; 22.53 %), highly (18,625 ha; 12.58 %), marginally (16,928 ha; 11.43 %) and not suitable (8,963 ha; 6.05 %) classes.

The municipal statistics quantify this geography and expose its asymmetries (Fig. 15-16). The not-suitable class is a corridor phenomenon: the five urbanized communes concentrate 2,461 ha (19.31 % of their 12,744 ha), against 4,139 ha (6.86 %) in the 60,304 ha of plain communes and 2,363 ha (3.15 %) in the 74,998 ha of Atlas communes, with communal maxima in Ouled Yaïch (448 ha; 32.0 %), Beni Mered (365 ha; 24.5 %) and Blida (1,183 ha; 22.3 %). Across municipalities this share varies inversely with communal area ($r = -0.61$), confirming that it traces built-up fabric rather than any biophysical gradient. The highly suitable class follows an opposite, agronomically unexpected gradient: it peaks in Chréa (2,737 ha; 34.1 %), Bouarfa (1,587 ha; 23.3 %), Djebabra (692 ha; 23.9 %), Souhane (1,325 ha; 18.5 %) and Chiffa (875 ha; 18.0 %), whereas plain communes range from 204 ha (4.7 %; Ben Khellil) to 1,061 ha (12.5 %; Larbaa); zone totals invert the expected order (Atlas 11,823 ha, 15.76 %; plain 5,675 ha, 9.41 %; corridor 1,127 ha, 8.84 %). The suitable class behaves as anticipated, forming the plain's matrix (28,130 ha; 46.65 %) and the Atlas valley floors (38,034 ha; 50.71 %), while the corridor retains only 4,015 ha (31.50 %) and displays the wilaya's most fragmented profile (marginally + moderately suitable = 40.35 %).

A fourth, finer pattern deserves mention. In the western and south-western communes (Oued Djer, El Affroun, Mouzaia), the map substitutes orange and yellow mottling for the plain's green matrix: marginally and moderately suitable land reaches 42.0 % (2,551 ha) in Oued Djer, 53.0 % (2,952 ha) in El Affroun and 43.3 % (3,620 ha) in Mouzaia, delineating the hilly transition between the Mitidja and the Chelif-margin reliefs, where rainfed cereals and scrub replace irrigated orchards. Within the green matrix itself, the scattered red speckle that textures the plain corresponds to hamlets,

farms and linear infrastructure, the municipal counterpart of the 13,912 ha (9.40 %) of built-up land recorded in the LULC criteria.

Three readings follow. The plain's suitable matrix is consistent with the intensive cropland of the Mitidja and with the documented peri-urban pressure on its eastern sector (Bellout et al., 2020). The corridor's not-suitable signal expresses land availability rather than capacity: the same communes still hold 4,015 ha of suitable land on some of the wilaya's best alluvial soils, so their low classes act as an artificial-surface mask superimposed on an otherwise favorable biophysical setting, a distinction land-evaluation theory requires to be kept explicit (FAO, 1976; Malczewski, 2004). The Atlas concentration of the top class is the most contestable feature of the map: with SMI and NDVI carrying 70.04 % of the total weight while terrain constraints enter only through the agro-physiographic factor (16.97 %, of which slope is 63.33 %, i.e. ≈10.7 % effective weight), moist, densely vegetated forest slopes score highest even where steep gradients preclude mechanized cropping; in a conservation landscape such as Chréa National Park, high NDVI and SMI values express ecosystem integrity rather than cropping capability. This inversion between plain and mountains is therefore best treated as a testable hypothesis of the weighting scheme, not as an established result.

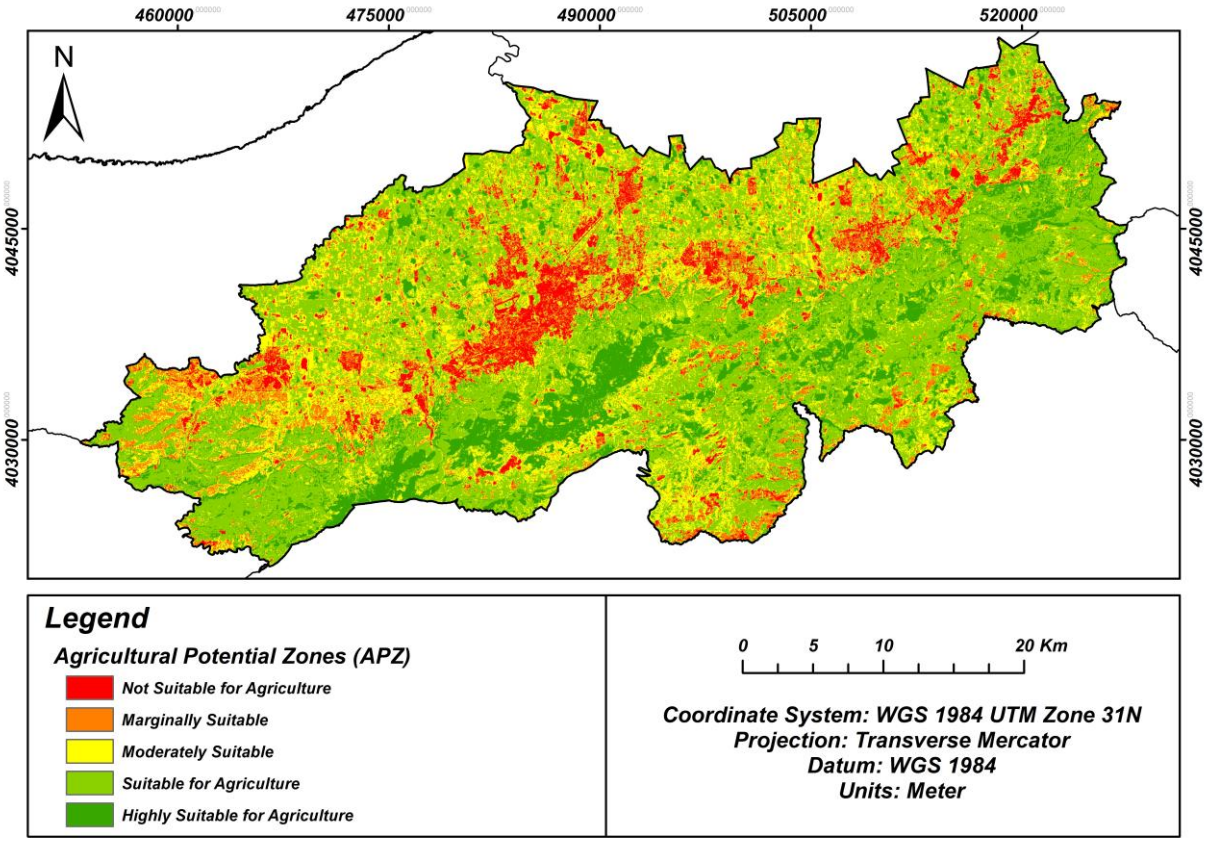


Fig. 14: Agricultural Potential Zones (APZ) Map.

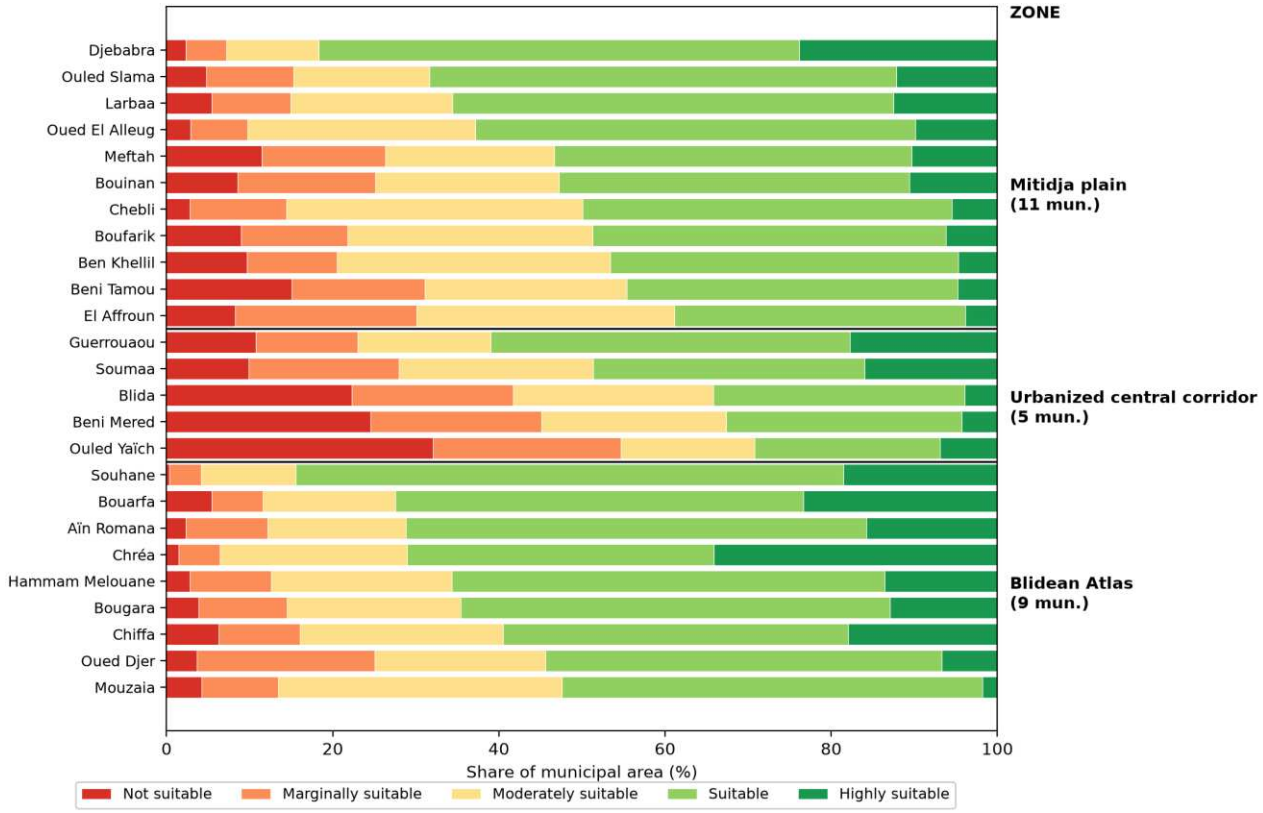


Fig. 15: Municipal distribution of the APZ Map.

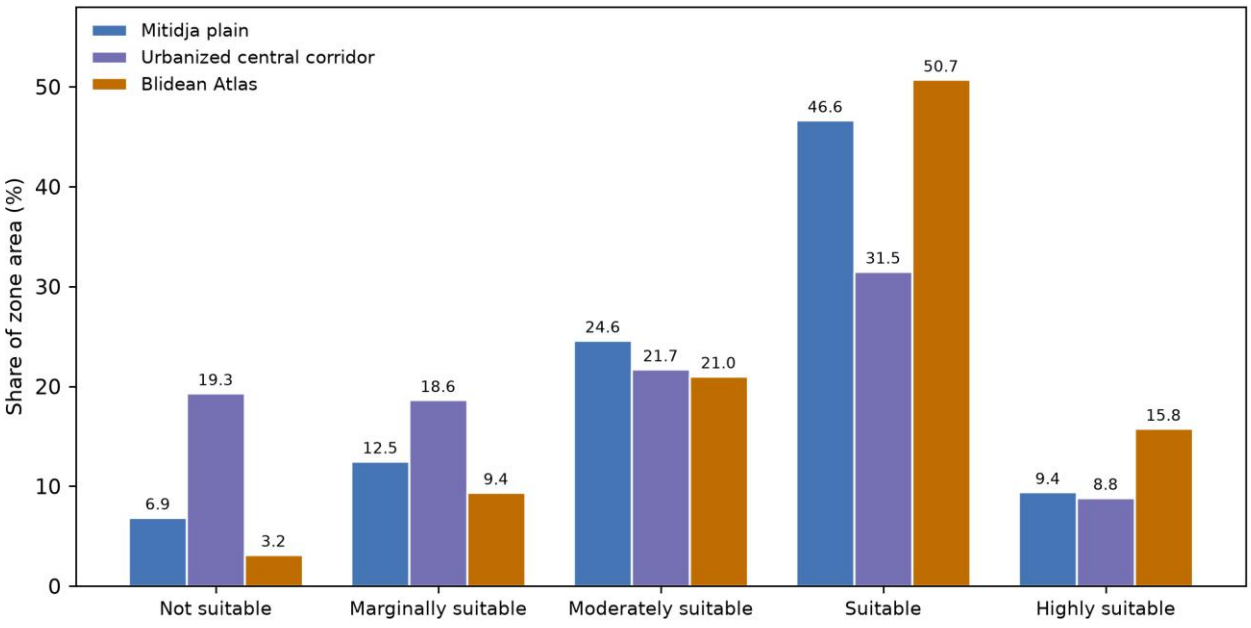


Fig. 16: Area-weighted APZ class composition of the three geographical zones.

Synthesis: what the validation demonstrates and what remains to be tested

The AUC of 0.935 demonstrates that the APZ index separates reference positives from negatives strongly and consistently across all four class thresholds, which supports the internal logic of the weighted combination and the usability of the map as a screening instrument for territorial planning. It does not, in its present aggregated form, establish per-class accuracy, statistical precision, or transferability beyond the calibration scene. Three developments would close these gaps: point-level reference data with spatially blocked cross-validation and bootstrap confidence intervals; a confusion-matrix accuracy assessment of the five classes; and one-at-a-time weight perturbation to test the stability of the Atlas top-class concentration. Crop-specific evaluations and multi-temporal SMI/NDVI composites would further

decouple transient vegetation state from enduring capability. The broader methodological lesson aligns with Mediterranean suitability studies in which moisture and vegetation indices dominate expert weightings (Faraslis et al., 2023; Zhu et al., 2022): high discrimination statistics certify that the index reproduces the environmental gradients its criteria encode, not that every gradient is agronomically meaningful at every elevation. For planning, the map already delivers two robust messages: the corridor's 4,015 ha of remaining suitable land is a finite reserve requiring explicit protection against the sprawl that accounts for the 2,461 ha of not-suitable land mapped in the same communes, and the plain's suitable matrix, not the mountain top class, is the agronomic backbone of the wilaya. Until the weighting hypothesis of the first section is tested, the highly suitable belt of the Blidean Atlas should be interpreted as an indicator of favorable moisture-vegetation conditions deserving conservation-oriented management, rather than as a mandate for agricultural intensification on steep terrain. Read together, the ROC diagnostic, the municipal statistics and the map itself thus provide a coherent, explicitly bounded evidence base: strong internal discrimination, a geographically legible class structure, and a clearly identified agenda of soil, temporal and field validation before the APZ map is used for crop-allocation decisions.

Conclusion

This study developed and validated an integrated GIS Remote Sensing and AHP framework for agricultural potential zoning in Blida Wilaya, northern Algeria, a representative semi-arid Mediterranean landscape subject to compounded climatic and urban pressures. Five spatial criteria: the Soil Moisture Index, NDVI, Land Surface Temperature, Land Use/Land Cover, and a composite Agro-Physiographic Suitability factor integrating slope, elevation, and distance from water bodies were harmonized at 30 m resolution, weighted through the AHP eigenvector method, and aggregated by weighted linear combination into a five-class Agricultural Potential Zone map.

The spatial configuration of the map is geographically coherent: the suitable class forms the agronomic matrix of the Mitidja plain and the intramontane valleys; the not-suitable class traces the urbanized piedmont corridor linking Blida, Ouled Yaïch, Beni Mered, Boufarik, Larbaa, and Meftah; and the highly suitable class concentrates along the Blidean Atlas front (Chréa, Hammam Melouane, Bougara) and the eastern hills (Djebabra, Souhane). ROC validation yielded an AUC of 0.935, confirming excellent discriminatory performance and supporting the map's usability as a screening instrument for territorial planning. Two robust planning messages follow: the 4,015 ha of suitable residual land within the urbanized corridor constitutes a finite reserve of prime alluvial soils requiring explicit protection against urban sprawl, and the plain's suitable matrix - rather than the mountain top class - is the agronomic backbone of the wilaya. The concentration of the highly suitable class in the Atlas should be interpreted cautiously, as it reflects a weighting scheme dominated by moisture and vegetation indices and may therefore signal ecosystem integrity and favorable hydro-vegetative conditions in forested terrain rather than mechanizable cropping capability; these areas merit conservation-oriented management until confirmed by field-level assessment.

Despite its strong internal discrimination, the model remains bounded by the aggregated form of its validation, and the per-class accuracy, statistical precision, and transferability of the APZ map beyond the calibration scene have yet to be established. Future work should incorporate point-level reference data with spatially blocked cross-validation and bootstrap confidence intervals, confusion-matrix accuracy assessment of the five suitability classes, and one-at-a-time weight perturbation to test the stability of the Atlas concentration, together with crop-specific evaluations and multi-temporal SMI/NDVI composites to decouple transient vegetation states from enduring land capability. Within these explicitly delimited bounds, the APZ map furnishes a transparent, reproducible, and geographically legible evidence base for sustainable agricultural land-use planning in Blida and, more broadly, in semi-arid Mediterranean regions of North Africa.

References

AbdelRahman, M. A. E., & Arafat, S. M. (2020). An approach of agricultural courses for soil conservation based on crop soil suitability using geomatics. Earth Systems and Environment, 4(1), 273–285. https://doi.org/10.1007/s41748-020-00145-x

Anusha, B. N., Raghu Babu, K., Pradeep Kumar, B., Padma Sree, P., Veeraswamy, G., Swarnapriya, C., & Rajasekhar, M. (2023). Integrated studies for land suitability analysis towards sustainable agricultural development in semi-arid regions of AP, India. Geosystems and Geoenvironment, 2(2), 100131. https://doi.org/10.1016/j.geogeo.2022.100131

Bellout, A., Vaz, E., & Penfound, E. (2020). Rethinking agricultural land use in Algiers: A spatial analysis of the Eastern Mitidja Plain. Habitat International, 104, 102239. https://doi.org/10.1016/j.habitatint.2020.102239

Binte Mostafiz, R., Noguchi, R., & Ahamed, T. (2021). Agricultural Land Suitability Assessment Using Satellite Remote Sensing-Derived Soil-Vegetation Indices. Land, 10(2), 223. https://doi.org/10.3390/land10020223

Cetin M, Isik Pekkan Ö, Ozenen Kavlak M, et al (2022) GIS-based forest fire risk determination for Milas district, Turkey. Natural Hazards. https://doi.org/10.1007/s11069-022-05601-7

Chemirik, C. H. K., Baahmed, D., Nedjai, R., Boudjemline, D. & Mahcer, I. (2024). Mapping Groundwater Potential Zones with GIS-RS-AHP Under Climate Change: Case of Mostaganem Plateau, Northwest Algeria. Ecological Engineering & Environmental Technology, 25(6), 72–89. https://doi.org/10.12912/27197050/186667

Choudhary, K., Boori, M. S., Shi, W., Valiev, A., & Kupriyanov, A. (2023). Agricultural land suitability assessment for sustainable development using remote sensing techniques with analytic hierarchy process. Remote Sensing Applications: Society and Environment, 32, 101051. https://doi.org/10.1016/j.rsase.2023.101051

Donmez, E., Yilmaz, M. T., & Yucel, I. (2024). Added utility of temperature zone information in remote sensing-based large scale crop mapping. Remote Sensing Applications: Society and Environment, 35, 101264. https://doi.org/10.1016/j.rsase.2024.101264

Escobar, M. T., Aguaron, J., & Moreno-Jimenez, J. M. (2004). A note on AHP group consistency for the row geometric mean priorization procedure. European Journal of Operational Research, 153(2), 318-322. https://doi.org/10.1016/S0377-2217(03)00166-0

ESRI (2016). ArcGIS Desktop: Release 10.8 Redlands, CA: Environmental Systems Research Institute.

FAO (1976). A Framework for Land Evaluation. FAO Soils Bulletin 32, Rome. https://www.fao.org/3/x5310e/x5310e00.htm

Faraslis, I., Dalezios, N. R., Alpanakis, N., Tziatzios, G. A., Spiliotopoulos, M., Sakellariou, S., Sidiropoulos, P., Dercas, N., Domínguez, A., Martínez-López, J. A., López-Urrea, R., Karam, F., Amami, H., & Nciri, R. (2023). Remotely Sensed Agroclimatic Classification and Zoning in Water-Limited Mediterranean Areas towards Sustainable Agriculture. Remote Sensing, 15(24), 5720. https://doi.org/10.3390/rs15245720

Jesus, j. B. D., & santana, i. D. M. (2017). Estimation of land surface temperature in caatinga area using landsat 8 data. Journal of Hyperspectral Remote Sensing, 7(3), 150–157. https://doi.org/10.29150/jhrs.v7.3.p150-157

Klein, J. (2019). Calculating the AHP priority vector. Software Engineering Institute, Carnegie Mellon University.

Madani AZ, Hermassi T, Taibi S, Dakhlaoui H and Mechergui M (2024) Climate change impacts on the Chiffa basin (northern Algeria) using bias-corrected RCM data. Front. Water 6:1507961. doi: 10.3389/frwa.2024.1507961

Machireddy, S. R. (2025). Geospatial technology approach for soil moisture estimation in Kurnool District, Andhra Pradesh, using NDVI and LST. Sensing and Imaging, 26(1), Article 62. https://doi.org/10.1007/s11220-025-00598-2

Malczewski, J. (2004). GIS-based land-use suitability analysis: A critical overview. Progress in Planning, 62(1), 3–65. https://doi.org/10.1016/j.progress.2003.09.002

Mihi, A., & Benaradj, A. (2022). Assessing and mapping wind erosion-prone areas in Northeastern Algeria using additive linear model, fuzzy logic, multicriteria, GIS, and remote sensing. Environmental Earth Sciences, 81, 47. https://doi.org/10.1007/s12665-021-10154-2

Mumcu Küçüker, D., & Cedano Giraldo, D. (2022). Assessment of soil erosion risk using an integrated approach of GIS and Analytic Hierarchy Process (AHP) in Erzurum, Türkiye. Ecological Informatics, 71, 101788. https://doi.org/10.1016/j.ecoinf.2022.101788

ONS – Office National des Statistiques (2008). Recensement Général de la Population et de l'Habitat 2008 (RGPH 2008). Algiers: ONS. https://www.ons.dz/spip.php?rubrique43

Saaty, T. L. (1977). A scaling method for priorities in hierarchical structures. Journal of Mathematical Psychology, 15(3), 234-281. https://doi.org/10.1016/0022-2496(77)90033-5

Saaty, T. L. (1980). The analytic hierarchy process: Planning, priority setting, resource allocation. McGraw-Hill.

Saaty, T. L. (1987). The analytic hierarchy process - what it is and how it is used. Mathematical Modelling, 9(3-5), 161-176.

Saaty, T. L. (1990). How to make a decision: The analytic hierarchy process. European Journal of Operational Research, 48(1), 9-26. https://doi.org/10.1016/0377-2217(90)90057-I

Saaty, T. L. (2003). Decision-making with the AHP: Why is the principal eigenvector necessary? European Journal of Operational Research, 145(1), 85-91. https://doi.org/10.1016/S0377-2217(02)00227-8

Saaty, T.L. (1980) The Analytic Hierarchy Process: Planning, Priority Setting, Resources Allocation. Mcgraw-Hill, New York.

Saha, A., Patil, M., Goyal, V. C., & Rathore, D. S. (2019). Assessment and Impact of Soil Moisture Index in Agricultural Drought Estimation Using Remote Sensing and GIS Techniques. Proceedings, 7(1), 2. https://doi.org/10.3390/ECWS-3-05802

Shinde, S. P., Barai, V. N., Gavit, B. K., et al. (2024). Assessment of groundwater potential zone mapping for semi-arid environment areas using AHP and MIF techniques. Environmental Sciences Europe, 36, 87. https://doi.org/10.1186/s12302-024-00906-9

NESCO-MAB (2025). Chréa Biosphere Reserve. UNESCO Man and the Biosphere Programme. https://www.unesco.org/en/mab/chrea

USGS - United States Geological Survey (2025). Digital Elevation Model (DEM) 30m × 30m resolution. Available at: https://earthexplorer.usgs.gov/. Last accessed: 20/11/2025

Wijesinghe, D. C. (2024). GIS-based AHP and MCDA Modeling for Cropland Suitability Analysis: A Bibliometric Analysis. Gazi University Journal of Science Part A: Engineering and Innovation, 11(3), 598-621. https://doi.org/10.54287/gujsa.1510527

Zhu, X., Xiao, G., & Wang, S. (2022). Suitability evaluation of potential arable land in the Mediterranean region. Journal of Environmental Management, 313, 115011. https://doi.org/10.1016/j.jenvman.2022.115011

Supplementary Files

This is a list of supplementary files associated with this preprint. Click to download.

- tab.1.docx
- tab.2.docx
- tab.3.docx